

# CHARACTERISATION OF DEFECTS IN ELECTRON IRRADIATED GA- OR B-DOPED CZ SILICON USING LAPLACE DLTS

P.N.K. Deenapanray<sup>1</sup>, Cloud Nyamhere<sup>2</sup>, F.D. Auret<sup>2</sup>

<sup>1</sup>Centre for Sustainable Energy Systems, FEIT, The Australian National University, Canberra ACT 0200, Australia, email: prakash.deenapanray@anu.edu.au

<sup>2</sup>Department of Physics, University of Pretoria, Pretoria 0002, South Africa, email: fauret@postino.up.ac.za

**ABSTRACT:** We have measured the electrical and annealing properties of defects created in Czochralski grown Si doped with either B or Ga by electron irradiation using both conventional and Laplace(L)-DLTS. With L-DLTS, we have been able to resolve several defects that cannot be resolved using conventional DLTS. L-DLTS provides a new avenue to study defect introduction rates and annealing kinetics in B- and Ga-doped Si. The isochronal annealing behaviour of the defects was also investigated.

**Keywords:** Defects, Laplace DLTS, Czochralski Si, Gallium doping

## 1 INTRODUCTION

Defects that introduce deep levels in the band gap of semiconductors, and which act as efficient recombination centres, have detrimental effects on the performance of solar cells. Defects can be created in a number of ways, including (1) growth of the semiconductor, (2) processing of device using low-energy particles (eg. plasma etching), and (3) under operating conditions. A notable example in the latter case is the degradation of the minority carrier lifetime of B-doped Cz Si solar cells under either illumination or carrier injection due to the formation of a metastable defect involving B and O [1]. The lifetime degradation is not observed in Ga-doped Cz Si [1]. However, few studies have investigated Ga-related defects in p-type Si, and detailed comparative studies of defect introduction rate of defects in B- or Ga-doped Cz Si are not numerous [2,3].

In this paper, we demonstrate that Laplace Deep Level Transient Spectroscopy (L-DLTS) provides the high resolution to study the electronic and annealing properties of discrete level defects that cannot be achieved using conventional DLTS [4]. We have used electron-irradiated B- or Ga-doped Cz Si as examples.

## 2 EXPERIMENTAL PROCEDURE

We have used B- and Ga-doped Cz Si with doping concentration of  $1.5 \times 10^{16} \text{ cm}^{-3}$  and  $3.5 \times 10^{16} \text{ cm}^{-3}$ , respectively. The samples were irradiated with 1 MeV electrons to fluences of  $1.5 \times 10^{16} \text{ cm}^{-2}$  (B-doped) or  $3.5 \times 10^{16} \text{ cm}^{-2}$  (Ga-doped), respectively, at room temperature. After chemical cleaning, circular Ti/Al Schottky diodes were fabricated on the irradiated side of the samples through a contact mask. Prior to electrical characterization, ohmic contacts were formed on the rear of samples using In-Ga eutectic. Isochronal annealing was performed on the Schottky diodes in the temperature range 30-300°C in steps of 50°C for 20 min in Ar. The samples were then characterized by current-voltage (I-V), capacitance-voltage (C-V), conventional (C-) and Laplace-DLTS. The “signatures” of defects (i.e. energy position in band gap relative to the valence band,  $E_t$ , and apparent capture cross-section,  $s_a$ ) were determined from Arrhenius plots of  $\ln(T^2/e_h)$  vs  $1000/T$ , where  $e_h$  is the hole emission rate and  $T$  is the measurement temperature.

## 3 RESULTS AND DISCUSSION

In this section, we discuss the electronic and annealing properties of hole traps created in the samples by electron-irradiation. First, it is enlightening to look at the defect resolution capability of Laplace over C-DLTS.

### 3.1 Conventional versus Laplace-DLTS

The C-DLTS spectrum measured from an electron-irradiated Ga-doped Cz sample irradiated and annealed at 150°C is shown in Fig. 1. The spectrum exhibits two broad peaks positioned around 112 K and 190 K that arise from overlapping defect peaks. This is evidenced by the shoulders on the high energy side of the two main peaks. On the other hand, the insets show the spectral density functions (SDF) – i.e. L-DLTS spectrum – measured around the peak positions of the two broad peaks. L-DLTS is clearly capable to resolve the broad DLTS peaks into two groups of discrete levels. Notably, the broad peak around 112 K is resolved into three discrete defects with levels at  $E_V + 0.18 \text{ eV}$ ,  $E_V + 0.17 \text{ eV}$ , and  $E_V + 0.13 \text{ eV}$ , while the peak around 190 K is resolved into two discrete defects with levels at  $E_V + 0.37 \text{ eV}$  and  $E_V + 0.33 \text{ eV}$ . In each inset, the peak at the lowest emission rate is an artifact of the algorithm used to extract the SDF from measured capacitance transients at constant temperature.

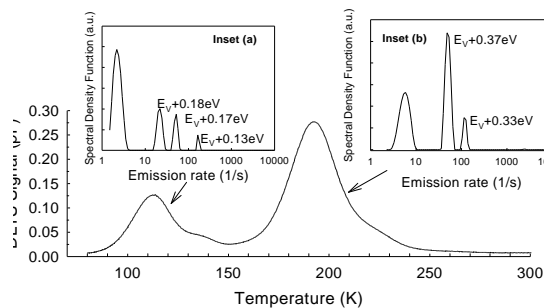


**Figure 1:** C-DLTS spectrum from electron-irradiated Ga-doped Cz Si and annealed at 150°C. The broad DLTS peaks are resolved by L-DLTS in the spectra shown in insets (a) and (b)

L-DLTS therefore provides a novel way to determine the electronic properties and annealing kinetics of otherwise overlapping discrete level defects either at all or more accurately. Similarly, it also allows the introduction rate of defects to be measured more realistically. This is especially important since Ga-doped Cz Si has been suggested to be more resistant to radiation damage than B-doped Cz Si. Yet previous studies have used C-DLTS [2,3] which, at best, can provide realistic measures of introduction rates only for the dominant defects. Further study is required to understand the effects of Ga atoms on the generation and removal of radiation-induced defects in Si [3]. The results presented here should be seen as a step forward in that direction.

### 3.2 Electronic properties of defects

We have determined the “signature” of electron-irradiation-induced defects in B- or Ga-doped Cz Si using Arrhenius plots of  $\ln(T^2/e_h)$  vs  $1000/T$ . Figure 2 shows the plots for defects observed in electron-irradiated B-doped Cz Si.

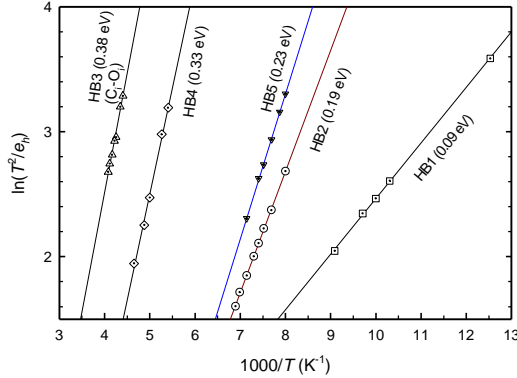


**Figure 2:** Arrhenius plots for defects in electron-irradiated B-doped Cz Si. These plots provide the “signatures” of defects

The “signatures” of defects created by irradiation in B- or Ga-doped Cz Si are summarized in Tables I and II, respectively. The tables provide a comparison between the energy positions of the defects as determined by both C- and L-DLTS. The last column of each table indicates the structure of the defects, where the question mark sign (i.e. “?”) refers to only a tentative assignment.

Defect	$E_t$ (eV)	$E_t$ (eV)	$s_a$ (cm <sup>2</sup> )	Defect structure
	C-DLTS	L-DLTS		
HB1	-----	0.09	$3.7 \times 10^{-20}$	-----
HB2	0.20	0.19	$3.2 \times 10^{-17}$	V-V [5]
HB3	0.29	0.33	$3.3 \times 10^{-16}$	C <sub>i</sub> -O <sub>i</sub> [6]
HB4	0.35	0.38	$3.7 \times 10^{-20}$	-----
HB5	-----	0.23	$2.7 \times 10^{-16}$	-----

**Table I:** Signature of defects in B-doped Cz Si

HB1, HB2 and HB3 are primary defects that are created during electron irradiation, and HB2 and HB3 can be attributed to the divacancy (V-V) [5] and the C<sub>i</sub>-O<sub>i</sub> complex [6]. HB4 and HB5 are secondary defects that are detected only after the irradiated samples have been annealed at 100°C. Secondary defects are generally created by the agglomeration of primary defects and/or

constituents thereof that become mobile at higher temperatures. C-DLTS was unable to measure the “signatures” of HB1 and HB5 in B-doped Cz Si.

The electronic properties of defects created in Ga-doped Cz-Si by electron irradiation were also determined for Arrhenius plots (not shown). They are summarized in Table II.

Defect	$E_t$ (eV)	$E_t$ (eV)	$s_a$ (cm <sup>2</sup> )	Defect structure
	C-DLTS	L-DLTS		
HG1_1	0.06	0.08	$4.4 \times 10^{-20}$	-----
HG1_2	0.13	0.11	$2.6 \times 10^{-21}$	-----
HG2_1	0.13	0.14	$5.1 \times 10^{-19}$	-----
HG2_2	0.23	0.17	$5.4 \times 10^{-21}$	-----
HG2_3	-----	0.18	$1.1 \times 10^{-19}$	? [2,3]
HG3_1	0.23	0.22	$1.4 \times 10^{-19}$	V-V [5]
HG3_2	0.31	0.34	$3.3 \times 10^{-16}$	-----
HG5	-----	0.37	$7.8 \times 10^{-16}$	C <sub>i</sub> -O <sub>i</sub> [6]
HG4	0.56	0.45	$7.7 \times 10^{-15}$	V-? [4]

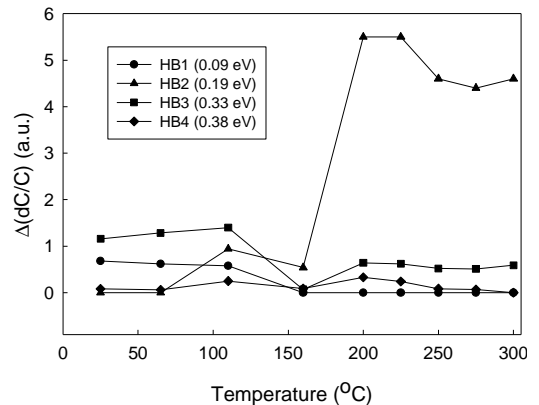
**Table II:** Signature of defects in Ga-doped Cz Si

A comparison between Tables I and II shows that a more extensive set of defects is introduced in Ga-doped Cz Si by electron irradiation. HG2\_3 is observed only after annealing at 150°C and more will be said about this defect later.

### 3.3 Annealing behaviour of defects in B-doped Cz Si

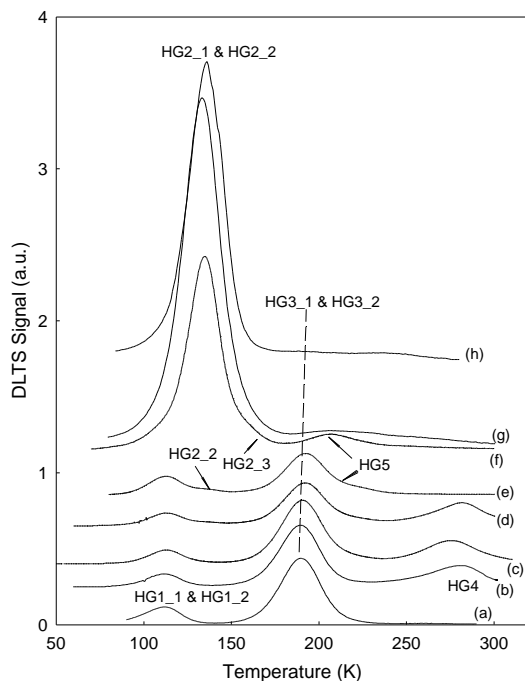
From a practical perspective, the complete characterization of defects requires that the annealing kinetics of the defects is established. Annealing experiments serve to determine, amongst others, (1) the temperature range within which a defect can be removed after its initial introduction, (2) whether secondary defects that may be detrimental to device performance are introduced during high-temperature steps in the processing of devices, and (3) the structure of defects through comparative studies. For instance, the electronic “signatures” of HG2\_3 and HG3\_1 may be similar, whereas their annealing behaviours are quite different. This subtle difference provides a versatile way to distinguish between them.

Figure 3 shows the isochronal annealing behaviour of defects in electron-irradiated B-doped Cz Si. Not shown is HB5 that was introduced after annealing at 100°C but was removed after annealing at 160°C. The peak defect intensity was measured from spectra taken by C-DLTS.



**Figure 3:** Isochronal annealing behaviour of defects in electron-irradiated Ga-doped Cz Si

The secondary defect HB4 is introduced above 100°C and it is completely removed at 300°C. HB3 ( $C_i-O_i$ ) showed an initial decrease around 160°C and thereafter underwent some reverse annealing. It was stable at the highest annealing temperature used in this study. A similar defect in [3] has been shown to exhibit reverse annealing properties, albeit at the higher temperature of 225°C, in heavy proton-irradiated samples [7]. The  $C_i-O_i$  complex is known to be thermally stable up to 400°C or 500°C in electron- or proton-irradiated samples [8]. HB1 that is thermally stable up to 160°C only has not previously been reported, most probably because of the lack of high-resolution DLTS. This defect could only be detected in our samples following L-DLTS measurements around the peak of HB2 observed with C-DLTS.



**Figure 4:** Defect evolution in electron-irradiated Ga-doped Cz Si after (a) irradiation at room temperature, and after post-irradiation annealing at (b) 60°C, (c) 80°C, (d) 100°C, (e) 150°C, (f) 200°C, (g) 250°C, and (h) 300°C

The most pertinent observation from Fig. 3 concerns the annealing behaviour of HB2. Figure 3 shows that the intensity of HB2, identified here as the divacancy, increased above 160°C – i.e. reverse annealing effect. HB2 is known to be annealed out at 300°C in electron-irradiated B-doped Cz Si without exhibiting any reverse annealing effect [8]. In heavy proton-irradiated Cz Si, the divacancy exhibited reverse annealing between 270-325°C [7]. The difference between the reverse annealing temperature reported here and in Ref [7] for V-V could be due to the use of different bombardment species and fluences used in the two investigations. Since HB2 is vacancy-related, the results shown in Fig. 3 suggest that there must be a release of vacancies from other sources around 160°C. There are two possible ways in which HB2 could grow. Single vacancies produced upon the dissociation of a complex could then agglomerate to form V-V. Alternatively, a defect complex such as V-V-X (X is an impurity), that

releases V-V directly upon dissociation. A deeper understanding of the exact mechanism contributing to the growth of HB1 is not clear to us at present, since this will require measurement of defects in the upper half of the band gap. Such measurements are currently underway as part of our initiative to determine the detailed annealing kinetics of defects in B- or Ga-doped Cz Si.

### 3.4 Annealing behaviour of defects in Ga-doped Cz Si

We now turn to the isochronal annealing behaviour of the hole traps observed in electron-irradiated Ga-doped Cz Si. Figure 4 shows the evolution of defects in as-irradiated Ga-doped Cz Si [spectrum (a)] and samples annealed at various temperatures [spectra (b) to (h)]. For convenience, like in the case of B-doped Cz Si, the spectra obtained using C-DLTS were used to monitor the annealing behaviour of defects. Figure 5 depicts the change in the peak intensity of the defects shown in Fig. 4 as a function of annealing temperature. Annealing of the combination of HG1\_1 and HG1\_2, which display similar electronic “signature” as HB1, also exhibits similar annealing characteristics.

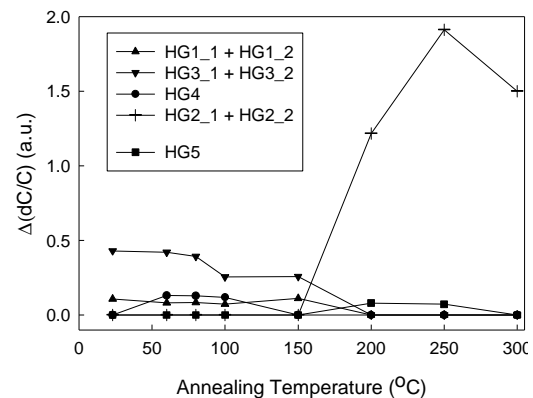


**Figure 5:** Isochronal annealing behaviour of defects in electron-irradiated Ga-doped Cz Si

There are a few notable differences between the annealing behaviour of defects in Ga-doped compared to B-doped Cz Si. The most pertinent one regards the behaviour of V-V that does not exhibit the reverse annealing effect. This suggests one of two scenarios, namely (1) that the source of vacancies present in B-doped Cz Si is not present in Ga-doped Cz Si, and/or (2) the release of vacancies, if this source were present, is preferentially scavenged by impurities like interstitial oxygen or oxygen dimers. Regarding the latter situation, it has been suggested that the formation of Gas-O<sub>2</sub>i defect is inhibited in Ga-doped Cz Si, which may imply a larger reservoir of interstitial oxygen to complex with vacancies released during annealing. Once, again one would have to monitor the annealing behaviour of the V-O centre ( $E_C - 0.18$  eV) to clarify this point. Another difference is the absence of  $C_i-O_i$  in the as-irradiated Ga-doped Cz Si. In fact,  $C_i-O_i$  is only observed after annealing at 200°C. This clearly reveals that the formation of this complex is inhibited in Ga-doped Cz Si, and is consistent with results previously reported in the literature [2,3].

Finally, the combination HG2\_1 & HG2\_2 is introduced by annealing at 150°C and, although it was

still stable at 300°C, its intensity was on the decrease. A defect with energy position at 0.18 eV relative to the valence band and displaying identical annealing behaviour has previously been reported in electron-irradiated Ga-doped Cz Si. This defect has been suggested to be a complex involving Ga<sub>i</sub> [2].

#### 4 SUMMARY

We have studied the electronic and annealing properties of defects created in B- or Ga-doped Cz Si by 1 MeV electron irradiation. In particular, we have shown that the better resolution of L-DLTS over C-DLTS provides a new way for the detailed characterization of defects in p-type Si. It has been shown that in B-doped Cz Si, the divacancy grows during annealing above 160°C. In contrast, the divacancy did not display the reverse annealing effect in Ga-doped Cz Si. There are other features of defect introduction and their annealing in Ga-doped Cz Si that are consistent with results previously reported in the literature. Our results reveal that further investigation has yet to be carried out on Ga-doped Cz Si in order to provide a complete picture of the properties of defects created in this material. We are currently measuring the detailed annealing kinetics of defects, as well as correlating the introduction rates of defects and free carrier compensation in the electron-irradiated samples using L-DLTS.

#### 5 ACKNOWLEDGEMENTS

PNKD acknowledges the financial support of the Australian Research Council. CN and FDA kindly acknowledge the National Research Foundation for financial assistance. Electron irradiations were performed at the Wright State University, USA.

#### 6 REFERENCES

- [1] J. Schmidt, K. Bothe, *Phys. Rev. B* 69 (2004) 024107.
- [2] A. Khan, M. Yamaguchi, Y. Ohshita, N. Dharmarasu, K. Araki, T. Abe, H. Itoh, T. Ohshima, M. Imaizumi, S. Matsuda, *J. Appl. Phys.* 90 (2001) 1170.
- [3] M. Yamaguchi, A. Khan, T. K. Vu, Y. Ohshota, T. Abe, *Physica B* 340-342 (2003) 596.
- [4] F.D. Auret, P.N.K. Deenapanray, *Critical Reviews in Solid State and Materials Sciences* 29 (2004) 1.
- [5] F. Volpi, A.R. Peaker, I. Berbezier, A. Ronda, *J. Appl. Phys.* 95 (2004) 4752.
- [6] G.L. Miller, D. Lang, L.C. Kimerling, *Ann. Rev. Mater. Sci.* 7 (1977) 377.
- [7] A. Khan, M. Yamaguchi, T. Hisamatsu, S. Matsuda, *J. Appl. Phys.* 87 (2000) 2162.
- [8] P.M. Mooney, L.J. Cheng, M. Süli, J.D. Gerson, J.W. Corbett, *Phys. Rev. B* 8 (1977) 3836.